

©2018. American Geophysical Union. All Rights Reserved

Access to this work was provided by the University of Maryland, Baltimore County (UMBC) ScholarWorks@UMBC digital repository on the Maryland Shared Open Access (MD-SOAR) platform.

**Please provide feedback**

Please support the ScholarWorks@UMBC repository by emailing [scholarworks-group@umbc.edu](mailto:scholarworks-group@umbc.edu) and telling us what having access to this work means to you and why it's important to you. Thank you.

# Validation of longwave atmospheric radiation models using Atmospheric Radiation Measurement data

Y. P. Zhou

Analytical Services & Materials, Inc., Hampton, Virginia

Robert D. Cess

Marine Sciences Research Center, State University of New York at Stony Brook, Stony Brook, New York

**Abstract.** Data taken at the Atmospheric Radiation Measurement Program's central facility in Oklahoma and processed as part of the Clouds and the Earth's Radiant Energy System–Atmospheric Radiation Measurement–Global Energy and Water Cycle Experiment (CAGEX) project have been used to validate the top-of-the-atmosphere and surface longwave radiative fluxes for two widely used radiation models: the Column Radiation Model from the National Center for Atmospheric Research Community Climate Model (CCM), and the Moderate Resolution Transmittance (MODTRAN3) radiation code. The results show that for clear skies the models slightly overestimate outgoing longwave radiation at the top of the atmosphere (OLR) and underestimate the surface downwelling longwave flux (SDLW). The accuracy of the radiation models is quite consistent with their respective levels of complexity. For MODTRAN3, for example, the OLR overestimate is  $7.1 \text{ Wm}^{-2}$  while the SDLW underestimate is  $4.2 \text{ Wm}^{-2}$ . For cloudy skies it is emphasized that the cloud input parameters, as determined from measurements by various instruments, require careful examination and preprocessing. Spatial and temporal averaging could result in the parameters representing different volumes of the atmosphere. The discrepancy between model calculations and observations is shown to be significantly reduced through the proper choice of input parameters.

## 1. Introduction

Theoretically based radiative transfer models are major tools used to study atmospheric radiative transfer processes associated with clouds. However, there are many uncertainties associated with cloud radiation parameterizations in current radiation models. While several recent studies have focused on the models' shortwave (SW) computation [e.g., Cess *et al.*, 1995; Chou and Zhao, 1997; Waliser *et al.*, 1996], it is equally important to realize that there are large uncertainties in the longwave (LW) calculations. For example, the Intercomparison of Radiation Codes in Climate Models (ICRCCM) found that for optically thin clouds the LW difference among models can be as large as  $30\text{--}80 \text{ Wm}^{-2}$  [Ellingson *et al.*, 1991], while a  $10\text{--}20 \text{ Wm}^{-2}$  discrepancy was found for the surface downward longwave radiation among several general circulation models (GCMs) and observations [Wild *et al.*, 1995]. It is essential that GCMs calculate the longwave flux correctly in order to project climate change caused by increasing greenhouse gases.

The validation of radiation models with in situ measurements requires concurrent input of the atmospheric state, including cloud information, which is itself difficult to access and subject to large uncertainty. Cloud microphysical properties are commonly estimated in terms of bulk cloud parameters measured using a variety of different instruments and techniques, and the input parameters required by different models are not always provided as needed by the observations. As will be demonstrated, this requires careful examination and collo-

cation of various parameters before the data can be used as input to the radiation models.

## 2. Data

The Clouds and the Earth's Radiant Energy System–Atmospheric Radiation Measurement–Global Energy and Water Cycle Experiment (CAGEX) project is a public access set of input data and radiative flux measurements over the Atmospheric Radiation Measurement (ARM) [Stokes and Schwartz, 1994] Southern Great Plains (SGP) cloud and radiation test bed (CART) site in Oklahoma [Charlock and Alberta, 1996] (see also the CAGEX home page, available from NASA Langley Research Center at <http://www-cagex.larc.nasa.gov/cagex>), in addition to providing calculated radiative fluxes using the Fu-Liou radiation code [Fu and Liou, 1992]. This data set provides a unique source for validating radiative transfer models, as well as for the intercomparison of different radiative transfer models.

Version 1 of CAGEX consists of data for a  $3 \times 3$  grid system, with each grid having a  $0.3^\circ$  resolution, every 30 min from 1409 to 2239 UTC for 26 days starting on April 5, 1994. The data include GOES satellite-based cloud properties [Minnis *et al.*, 1995], atmospheric soundings, and other input parameters that are needed for broadband radiative transfer calculations. The validation data include surface SW (pyrheliometer and pyranometer) and LW (pyrgeometer) fluxes, plus GOES measurements of the time of arrival (TOA) broadband LW fluxes and broadband SW albedos [Minnis *et al.*, 1995]. The vertical profiles of broadband shortwave and longwave fluxes were calculated using the Fu-Liou radiation code [Fu and Liou, 1992]. In the present work, calculations

Copyright 2000 by the American Geophysical Union.

Paper number 2000JD900557.  
0148-0227/00/2000JD900557\$09.00

using additional radiative transfer models are performed for the central facility (CF), where the soundings and surface radiometric measurements were taken, and the LW fluxes at the surface and at the TOA are analyzed and compared.

### 3. Radiation Models

Two widely used radiation models are employed in this study: the National Center for Atmospheric Research Community Climate Model (CCM2-CCM3) Column Radiation Model (CRM) and the Moderate Resolution Transmittance (MODTRAN) radiation model. The two models vary in their sophistication and general applications. The CRM is a stand-alone version of the radiation model used in the NCAR Community Climate Models (CCM2 and CCM3) and is composed of the actual subroutines from the CCM, which have been modified as little as possible in order to run in a stand-alone mode (see the CRM home page, available from Climate and Global Dynamics Division, University Corporation for Atmospheric Research, at <http://www.cgd.ucar.edu/cms/crm/>). The longwave radiative transfer in the CRM is based on the absorptivity-emissivity formulation of *Ramanathan and Downey* [1986]. Major absorbers include  $\text{H}_2\text{O}$  [*Ramanathan and Downey*, 1986], the  $15\text{ }\mu\text{m}$  band system of  $\text{CO}_2$  [*Kiehl and Briegleb*, 1991], and the  $9.6\text{ }\mu\text{m}$  band system of  $\text{O}_3$  [*Ramanathan and Dickinson*, 1979]. Although clouds are diagnosed by *Slingo's* [1987] scheme in the original CCM, the CRM uses cloud amount and liquid water content as inputs and, thus, is independent of the convection and cloud schemes in the CCM. Cloud emissivity is accounted for by an effective cloud amount, which is a function of liquid water content at each model layer. No ice clouds are present in the CCM2 version, but they are present in the CCM3 version.

Minor trace gases ( $\text{CH}_4$ ,  $\text{N}_2\text{O}$ , CFC-11, and CFC-12) have been incorporated into the CCM3 CRM. CCM3 differentiates the cloud drop size for clouds over maritime and continental regions [*Kiehl et al.*, 1994]. The amount of ice particles in the total cloud water is specified when the temperature is below  $-10^\circ\text{C}$ , and cloud absorption by ice particles is considered differently from that by cloud liquid droplets [*Kiehl et al.*, 1996]. For this study the model's vertical resolution has been changed from 18 to 48 layers to fit the CAGEX input data. The difference in broadband TOA and surface longwave fluxes between these two model resolutions was found to be less than  $1\text{ Wm}^{-2}$ .

The MODTRAN code is a band model which calculates atmospheric radiance and transmittance for wavenumbers from 0 to  $50,000\text{ cm}^{-1}$  at a nominal spectral resolution of  $2\text{ cm}^{-1}$  [*Abreu and Anderson*, 1996], and it was developed from the Low Resolution Transmittance code (LOWTRAN) [*Kneizys et al.*, 1988]. Version 3 of MODTRAN, MODTRAN3, encompasses all the capabilities of LOWTRAN and contains features that many other models do not incorporate, including a Voigt line shape through parameterization of the transmittance to line-by-line calculations, internal aerosols, cloud models, and default atmospheric profiles [*Abreu and Anderson*, 1996]. Model parameters are derived directly from the HITRAN 1992 database [*Rothman et al.*, 1992]. The version used in this study is MODTRAN3.7, which has a major upgrade so that users can easily define cloud descriptions. For example, clouds can be placed anywhere within the defined atmosphere,

can coexist with aerosols, and can have a mixed phase composition [*Acharya et al.*, 1998].

The Fu-Liou [*Fu and Liou*, 1992] radiation code was used by CAGEX to produce surface and atmospheric radiative fluxes at the ARM SGP CART site. It is a plane-parallel,  $\delta$ -four-stream code using a correlated- $k$  distribution method for gaseous transmission. Scattering is treated in the SW as well as the LW. The code accounts for the radiative effects of  $\text{H}_2\text{O}$ ,  $\text{CO}_2$ ,  $\text{O}_3$ ,  $\text{O}_2$ ,  $\text{CH}_4$ ,  $\text{N}_2\text{O}$ , Rayleigh scattering, aerosols, liquid water droplets, hexagonal ice crystals, and spectrally dependent surface reflectivity. Twelve spectral intervals are used in the LW ( $2200\text{--}1\text{ cm}^{-1}$ ). Continuum absorption of  $\text{H}_2\text{O}$  [*Roberts et al.*, 1976] is included ( $280\text{--}1250\text{ cm}^{-1}$ ). The uniform mixing ratios for  $\text{CO}_2$ ,  $\text{CH}_4$ , and  $\text{N}_2\text{O}$  are 330, 1.6, and 0.28 ppmv, respectively. We have used the same  $\text{CO}_2$  mixing ratio in the CRMs and MODTRAN3, and essentially the same  $\text{CH}_4$  and  $\text{N}_2\text{O}$  mixing ratios. A minor exception in the latter two cases is that the CRMs and MODTRAN3 use a variable mixing ratio in the stratosphere and the MODTRAN3  $\text{CH}_4$  and  $\text{N}_2\text{O}$  mixing ratios change slightly in the tropical atmosphere. Calculations using the Fu-Liou code are taken directly from CAGEX for comparison with the CRM and MODTRAN3 results.

The four models differ in aerosol treatment. The CRMs do not include aerosols in the LW calculations, while CAGEX used the optical depth inferred from the Multi-Filter Rotating Shadowband Radiometer (MFRSR) measurements at five SW bands ( $0.412$ ,  $0.498$ ,  $0.606$ ,  $0.663$ , and  $0.856\text{ }\mu\text{m}$ ). The optical depths for the Fu-Liou code, as used in CAGEX, were interpolated into the CAGEX spectrum (6 SW bands and 12 LW bands) with the aid of *d'Almeida et al.'s* [1991] table of wavelength and relative humidity-dependent aerosol optical parameters and were apportioned with altitude using *Spinhirne's* [1993] vertical distribution expression. The accuracy of the retrieved aerosol optical depths from MFRSR was estimated to be around 5–10% [*Charlock and Alberta*, 1996]. To address the importance of whether a model does or does not include aerosols in its LW calculations, we have performed several aerosol sensitivity studies with MODTRAN3, including using aerosols similar to those modeled by CAGEX. We found that inclusion of aerosols within the model should increase SDLW by  $\sim 1\text{--}3\text{ Wm}^{-2}$  and reduce OLR by  $\sim 0.4\text{--}1.0\text{ Wm}^{-2}$ , depending upon the type of aerosol. As we emphasize in section 4, these effects will not substantially impact our comparisons.

The models likewise differ in their treatment of scattering for cloudy sky conditions. The CRMs neglect LW scattering by clouds, while this is included in both the Fu-Liou model and in MODTRAN3. As demonstrated by *Fu et al.* [1997], the neglect of scattering in the infrared can cause an overestimate in OLR of  $\sim 6\text{ Wm}^{-2}$  for the cloudy sky conditions that they considered.

### 4. Clear-Sky Validation

Before addressing the issue of clouds we first consider clear skies. The clear-sky input temperature and humidity profiles are taken from the CAGEX Mesoscale Analysis and Prediction System (MAPS) soundings, which are based on balloon-borne soundings every 3 hours for the ARM SGP CF and for the April 1994 Intensive Observational Period (IOP). The MAPS profiles use balloon soundings for lower level temperatures (from surface to 100 mbar) and humidities (from surface to 300 mbar), and the Television Infrared Observation Satellite (TIROS) Operational Vertical Sounder (TOVS) [*Susskind et al.*, 1997] for upper level temperature ( $70\text{--}0.4$

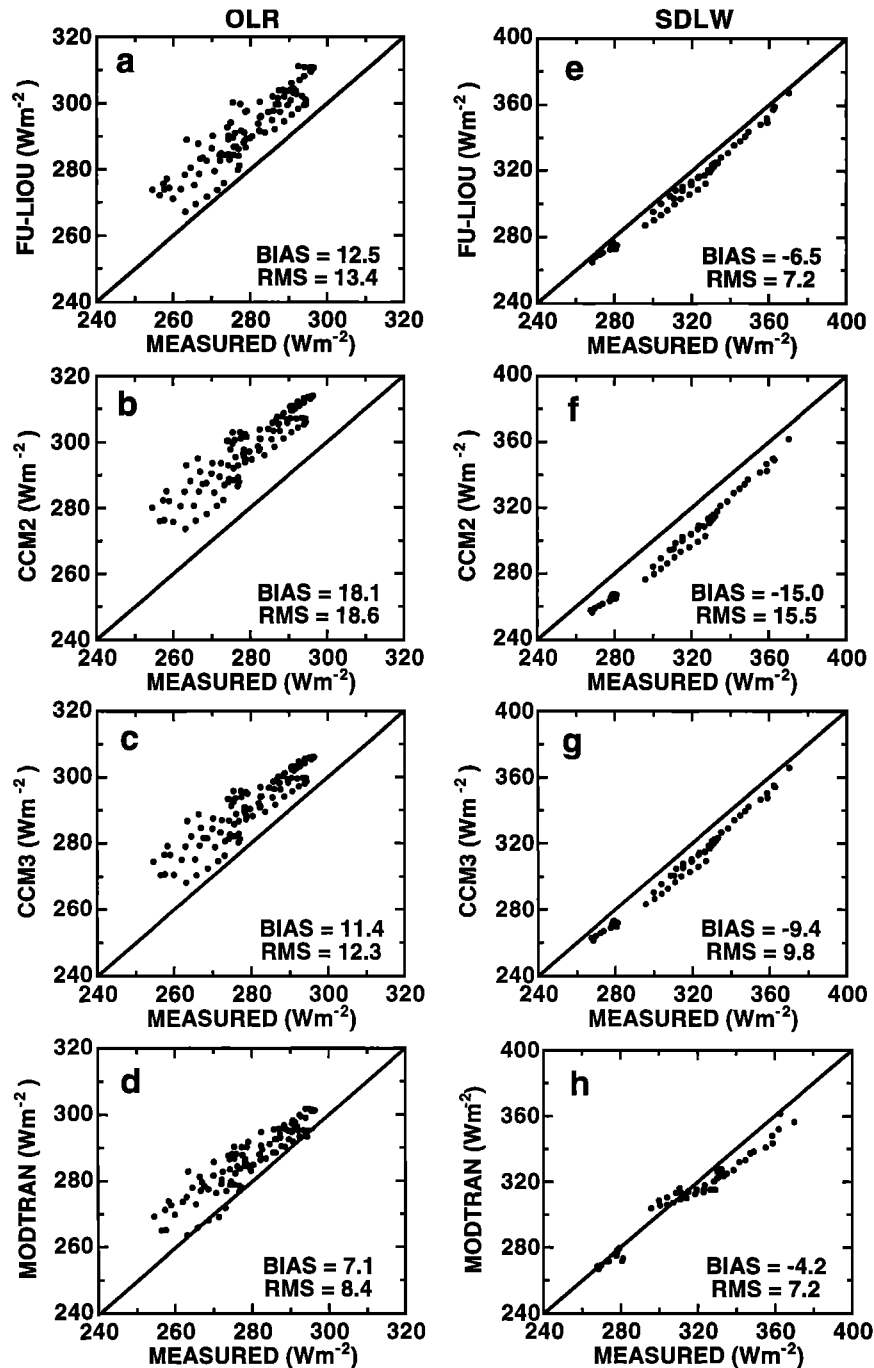


**Figure 1.** (a) Clear-sky OLR as determined from the Fu-Liou model compared to the measured clear-sky OLR. (b) Same as Figure 1a but for the CCM2 CRM. (c) Same as Figure 1a but for the CCM3 CRM. (d) Same as Figure 1a but for MODTRAN. (e) Clear-sky SDLW as determined from the Fu-Liou model compared to the measured clear-sky SDLW. (f) Same as Figure 1e but for the CCM2 CRM. (g) Same as Figure 1e but for the CCM3 CRM. (h) Same as Figure 1e but for MODTRAN.

mbar). Climatological humidity is adopted for upper level humidity. Ozone data are from the solar backscattered ultraviolet (SBUV2) product. MAPS soundings were interpolated vertically and temporally to the CAGEX grid system.

Figure 1 shows scatterplots of the model calculations versus measurements for the clear-sky OLR and SDLW, with the Fu-Liou model calculations from CAGEX [Charlock and Alberta, 1996] also shown for comparative purposes. The models' surface upwelling longwave flux adopts radiometric measure-

ments so as to avoid the uncertainty associated with surface skin temperature and emissivity, and the clear-sky identification is from GOES. A total of 101 clear-sky soundings are available for use in the calculations, but only 57 SDLW measurements are available because of missing SDLW data. All four models produce OLR fluxes that are higher than the GOES measurements, while their SDLW fluxes are lower than the surface pygeometer measurements, with the CCM2 CRM having the largest and MODTRAN3 having the smallest

biases. The smaller bias for the CCM3 CRM, relative to that for CCM2, is consistent with the improvement of CCM3 CRM by inclusion of minor trace gases, so that the non-CO<sub>2</sub> trace gases produce about a 6–7 Wm<sup>-2</sup> difference in both OLR and SDLW, which is close to the 5 Wm<sup>-2</sup> estimate of *Slingo and Webb* [1992]. The Fu-Liou radiation model has taken account of the radiative effects of H<sub>2</sub>O, CO<sub>2</sub>, O<sub>3</sub>, CH<sub>4</sub>, and N<sub>2</sub>O. CFCs are not included, but CFC radiative forcing is reported to be less than 1 Wm<sup>-2</sup> [Charlock and Alberta, 1996]. MODTRAN3 includes most of the absorbing gases, including H<sub>2</sub>O, CO<sub>2</sub>, O<sub>3</sub>, N<sub>2</sub>O, CO, CH<sub>4</sub>, NO, SO<sub>2</sub>, NO<sub>2</sub>, NH<sub>3</sub>, HNO<sub>3</sub>, and CFCs.

The overall overestimation of OLR and underestimation of SDLW for all the models could be caused by a systematic underestimate of the models' gaseous absorption. Also, as suggested in CAGEX [Charlock and Alberta, 1996], the biases of SDLW and OLR may come from quite different sources. For example, the underestimate of SDLW may be due to insufficient absorption by the water vapor continuum, while the overestimate of OLR could be caused by inaccurate upper atmosphere soundings. For MODTRAN3, which includes a new and improved water vapor continuum, the minimal biases in OLR and SDLW (relative biases of 2.5% and -1.3%, respectively) do not appear to be related to the background aerosol used in that model. As discussed in section 3, we have performed sensitivity studies which show that aerosols impact SDLW much more than OLR, while MODTRAN3 has a larger OLR bias than SDLW bias. Also, recall that these sensitivity studies show that inclusion of aerosols within a model should increase SDLW by ~1–3 Wm<sup>-2</sup> and reduce OLR by ~0.4–1.0 Wm<sup>-2</sup>. These effects will not substantially impact the results shown in Figure 1.

That the models systematically overestimate the OLR does not appear to be an artifact of the GOES OLR measurements. As demonstrated through a number of independent checks [Doelling et al., 1999], the GOES OLR is consistent with other measurements. These checks included comparisons with measurements made by the wide field of view (WFOV) instrument on board the Earth Radiation Budget Satellite (ERBS) [Smith et al., 1986], measurements made by the Scanner for Radiation Budget (ScaRaB) [Kandel et al., 1993], and measurements performed as part of Clouds and the Earth's Radiant Energy System (CERES) [Wielicki and the CERES Science Team, 1995]. Compared to the ERBS WFOV measurements during eight months between 1994 and 1998, the GOES OLR showed a positive bias of only 0.3 Wm<sup>-2</sup>, while the ScaRaB comparison showed GOES OLR biases of only -1 Wm<sup>-2</sup> for April 1994 and 1.3 Wm<sup>-2</sup> for July 1994. The CERES comparison was for January 1998, for which the GOES OLR bias was 3.2 Wm<sup>-2</sup>. This comparison, however, used the original CERES values before the spectral corrections were applied, and it is anticipated that the GOES CERES bias of 3.2 Wm<sup>-2</sup> will be reduced when the revised CERES data are used (P. Minnis, private communication, 2000). The systematic underestimate of the models does not appear to be an artifact of the SDLW as measured by the surface pyrgeometer either. As demonstrated by Han and Ellingson [2000], the pyrgeometer measurements were in good agreement with observations from the adjacent atmospheric emitted radiance interferometer (AERI). There were only small steady biases between them, with the pyrgeometer measuring 1–4 Wm<sup>-2</sup> less than the AERI-based fluxes.

## 5. Cloudy Sky Validation

### 5.1. Cloud Input Parameters

How to input the correct cloud information into a radiation model is by no means straightforward. ARM has several direct cloud observation systems as well as the satellite-retrieved cloud products. CAGEX used the cloud products derived from the GOES satellite [Minnis et al., 1995] in their calculations, and these include cloud amount, height, optical depth, emissivity, and reflectance for the following three height intervals: low (<2 km), middle (2–6 km), and high (>6 km). The technique used is the Layered Bispectral Thresholding Method (LBTM), using radiance measurements at one visible channel and one infrared channel, and it is based on the assumptions of plane-parallel and nonoverlapping clouds. Since the satellite only sees one layer of clouds for each individual pixel, there may be substantial problems for the lower clouds when overlapping multilayer clouds exist. The cloud amount is the percentage of cloudy pixels relative to all the pixels of the grid, and the cloud properties are essentially spatial averages of the cloudy pixels for each layer.

An important question is whether spatially averaged cloud properties are also representative of the average cloud status in a temporal context, since model calculations will be compared with the surface radiometric observations which are processed as temporal averages from temporally continuous measurements at the same point. For SW radiation the equivalence of spatial and temporal averaging has been discussed in two studies. Cess et al. [1996] indirectly compared atmospheric transmittance from a temporal average of measurements of one pyranometer with a spatial average of a close network of 11 pyranometers in Wisconsin with respect to the regression of the TOA albedo versus atmospheric transmittance. Close agreement with the 11-station network was obtained when the surface averaging time, for a single station, was ~40 min. Correspondingly, Long and Ackerman [1995] found that the correlation of any pair of surface pyranometers increased monotonically with averaging time for the same Wisconsin network. Both papers thus demonstrated the equivalence of temporal and spatial averaging in a statistical sense, and their measurements were for SW only. Neither study, however, directly compared a single parameter observed from both a surface instrument and a satellite.

Cloud amount and cloud base height determined from instantaneous half-hour satellite measurements have correspondingly been compared with the 1 min surface micropulse lidar measurements. The satellite cloud amount is defined as the percentage of cloudy pixels, relative to all pixels, within the 0.3° × 0.3° grid, while cloud base height is the cloud amount weighted average of high-level, midlevel, and low-level cloud bases. The surface measurements have been averaged from 10 to 60 min, each centered at the TOA sampling time. The surface cloud amount is defined as the percentage of overcast samples, relative to total samples, in the averaging time period, and the cloud base height is the average base of the overcast samples. From Figure 2 the differences between the surface lidar measurements and the satellite measurements are substantial. The large RMS for both parameters, which is relatively insensitive to the averaging period, and which actually increases with increasing averaging time for the cloud base height, indicates that the individual surface and satellite measurements are not in good agreement, irrespective of the averaging period of the surface measurements. Although it is

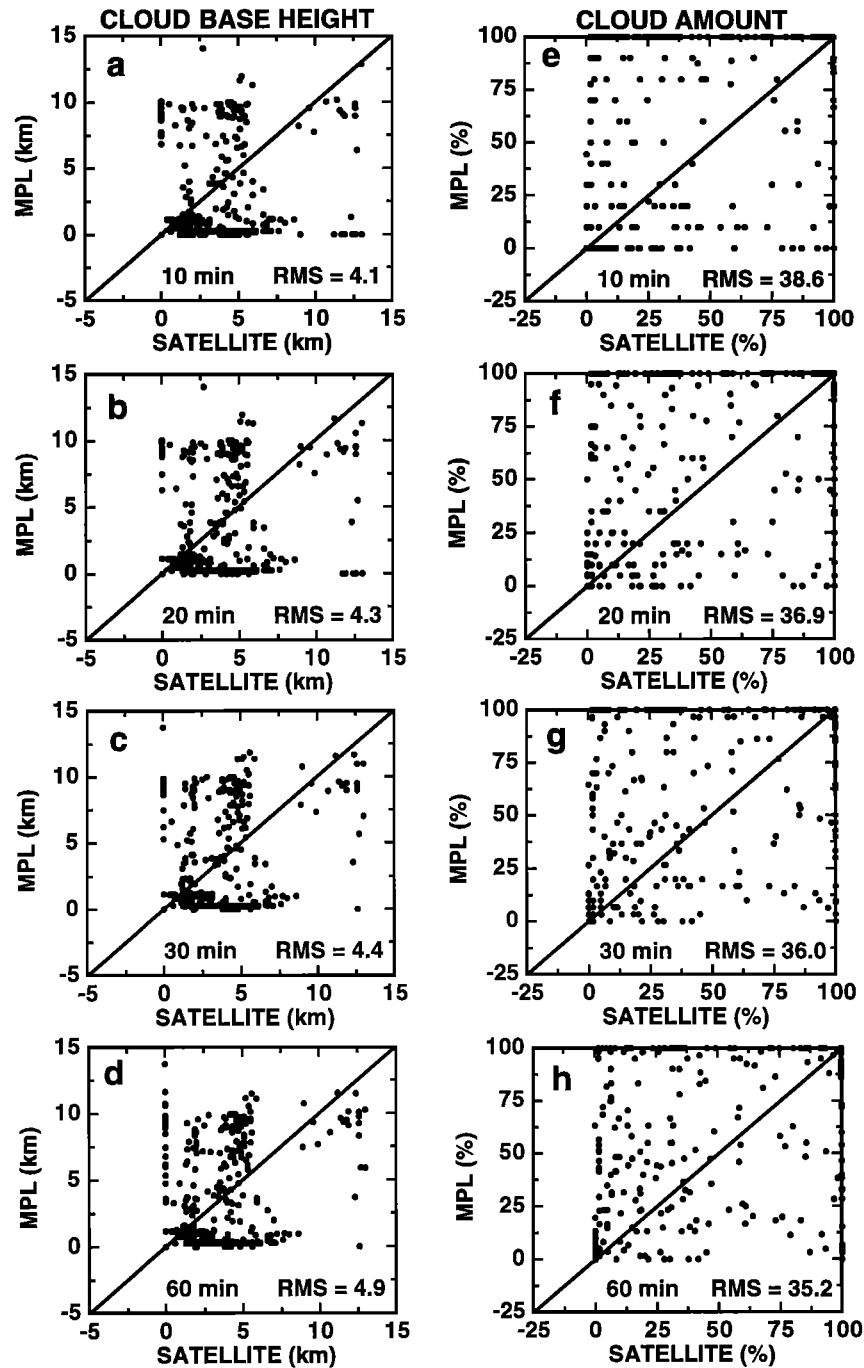


**Figure 2.** (a) Cloud-based height measured from the surface with the micropulse radiometer (MPL) and averaged over 10 min, compared to the cloud base height measured by the satellite. (b) Same as Figure 2a but with the MPL measurements averaged over 20 min. (c) Same as Figure 2a but with the MPL measurements averaged over 30 min. (d) Same as Figure 2a but with the MPL measurements averaged over 60 min. (e) Cloud amount measured from the surface with the micropulse radiometer and averaged over 10 min, compared to the cloud amount measured by the satellite. (f) Same as Figure 2e but with the MPL measurements averaged over 20 min. (g) Same as Figure 2e but with the MPL measurements averaged over 30 min. (h) Same as Figure 2e but with the MPL measurements averaged over 60 min.

generally felt that satellite measurements give the most accurate cloud amount information, while the lidar measurements are preferable for cloud base height, for multilayer clouds the lidar can only provide the cloud base of the lowest cloud layer.

It is also important to note that the observed cloud parameters can be quite different from the model-required input

parameters. Moreover, since the cloud parameterizations and input requirements for the CCM2-CCM3 CRM are quite different than for MODTRAN3, the input parameters need to be treated accordingly with respect to the two models. In sections 5.2 and 5.4 we discuss the treatment of the two models separately.

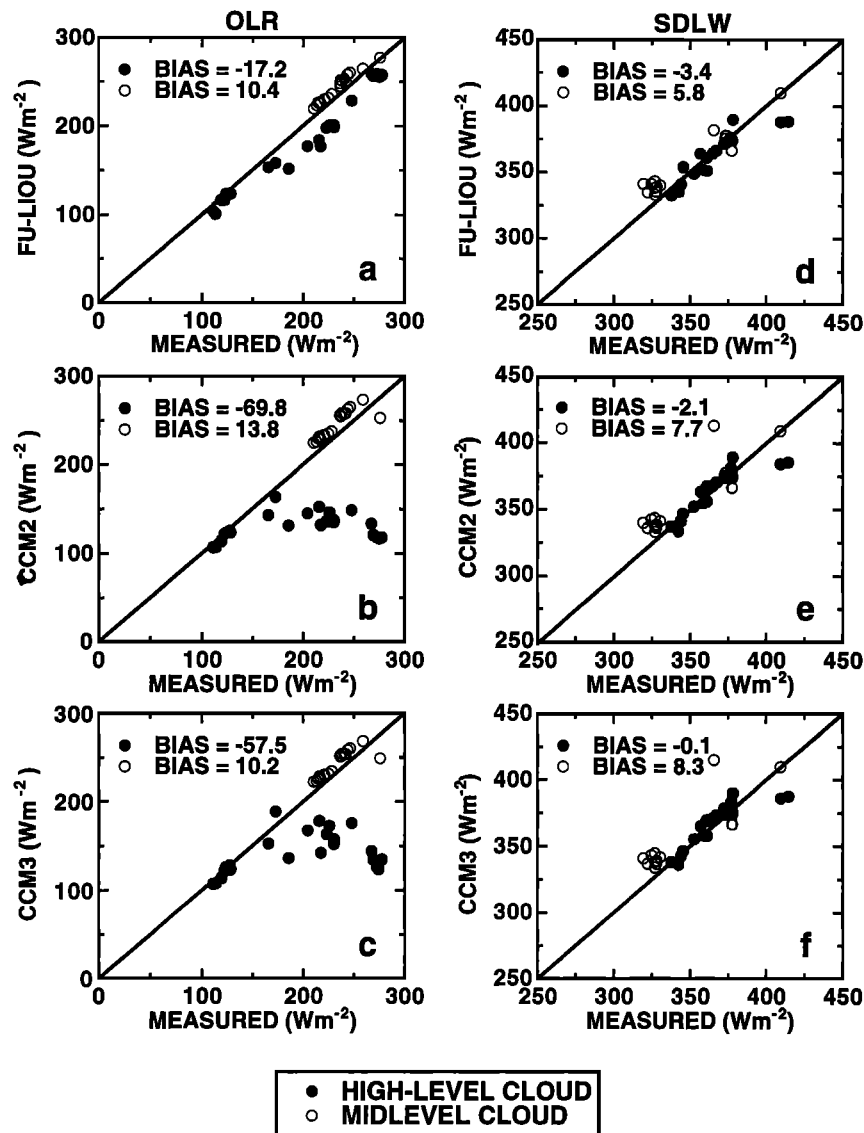


**Figure 3.** (a) OLR as determined from the Fu-Liou model, for cloudy sky soundings and a one-layer satellite cloud, compared to the measured OLR. (b) Same as Figure 3a but for the CCM2 CRM. (c) Same as Figure 3a but for the CCM3 CRM. (d) SDLW as determined from the Fu-Liou model, for cloudy sky soundings and a one-layer satellite cloud, compared to the measured SDLW. (e) Same as Figure 3d but for the CCM2 CRM. (f) Same as Figure 3d but for the CCM3 CRM.

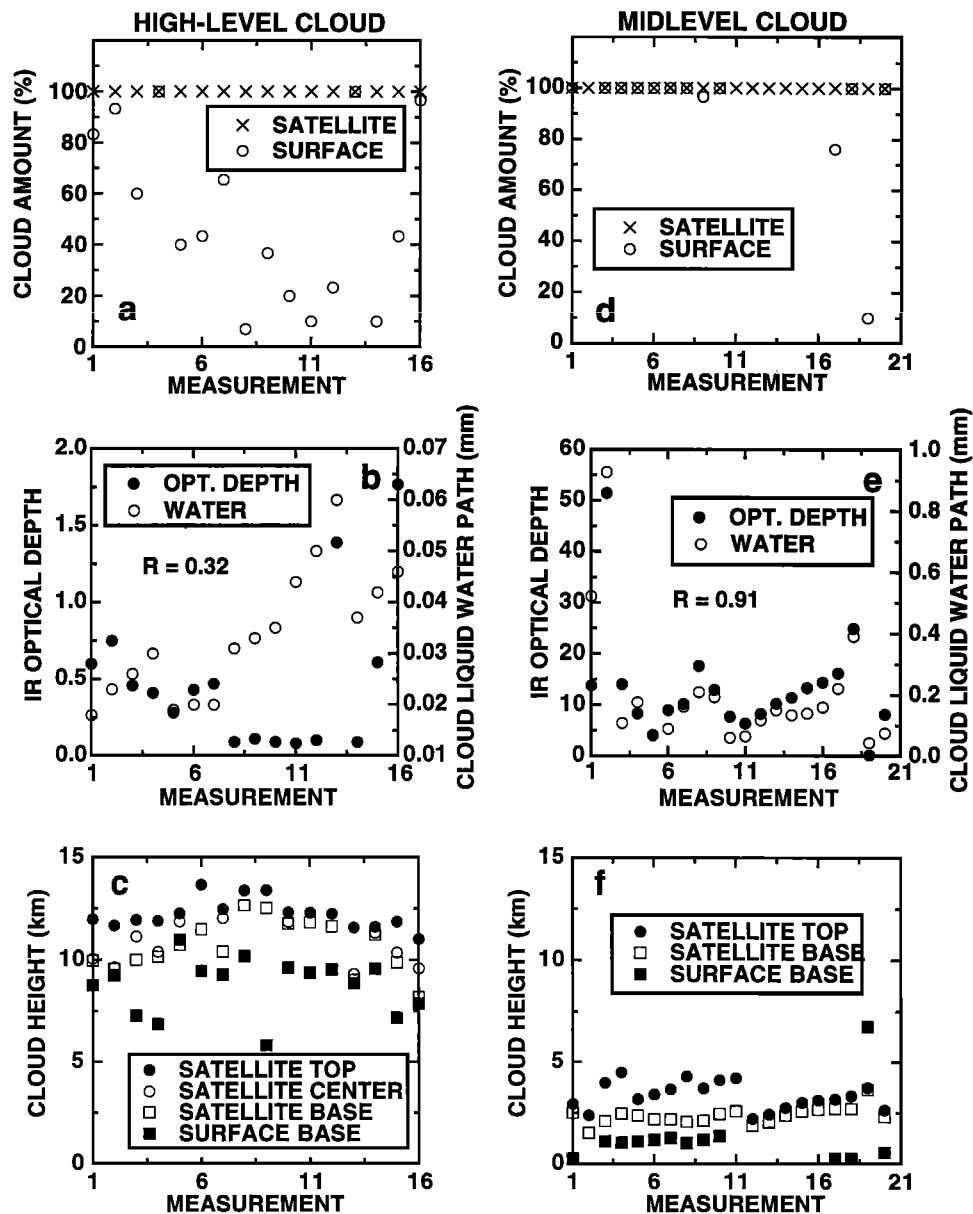
## 5.2. CCM2-CCM3 CRM: One-Layer Satellite Cloud

We have chosen to first study the one-layer overcast cloud (low-level, midlevel, or high-level) as seen from the satellite to initially simplify the problem. The CCM2-CCM3 CRMs require input of cloud amount and liquid-ice water content for each model cloud layer. Since a one-layer satellite-observed cloud can actually occupy several model layers, we assume 100% cloud amount for each model layer between the satellite-determined cloud base and cloud top, with the physical (i.e., actual) cloud top used in the present calculations. The in situ total cloud liquid water, as measured by the surface microwave radiometer, was then distributed among the model cloud layers with a weight proportional to the layer mass.

Figure 3 shows the results for the satellite one-layer overcast cloud conditions. Again, the Fu-Liou model calculations from CAGEX [Charlock and Alberta, 1996] are shown for comparative purposes, although, as will be discussed in section 5.2.2,

their cloud liquid water was inverted from GOES observations of the visible cloud optical depth, rather than determined from the surface microwave radiometer measurements. The solid circles and open circles represent the one-layer high-level and midlevel clouds, respectively. The one-layer low-level clouds are not shown since there are too few samples. For the one-layer midlevel clouds the models show good agreement with each other to within  $4 \text{ Wm}^{-2}$  for both OLR and SDLW, and likewise reasonable agreement with the measurements. For high-level clouds the models are again in good agreement with the measurements for SDLW (Figures 3d–3f). Conversely, the models show large discrepancies from the measurements of OLR from about  $-17 \text{ Wm}^{-2}$  in the Fu-Liou model to  $-70 \text{ Wm}^{-2}$  for the CCM2 CRM (Figures 3a–3c).

In order to identify the cause for these large biases in OLR the cloud amount, height, IR optical depth, and total liquid water path were examined for the individual measurements in



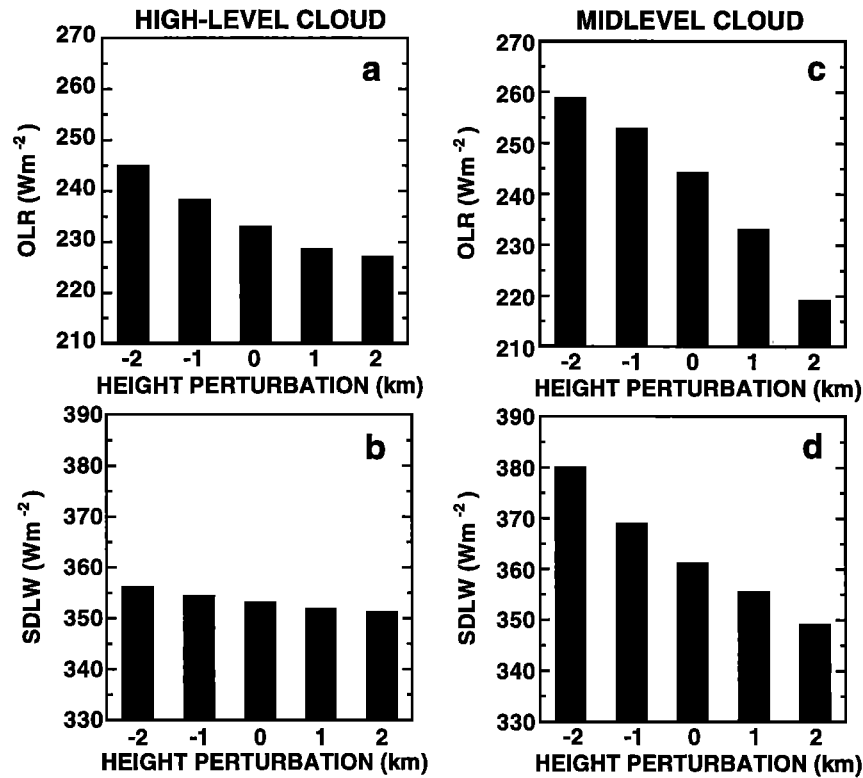
**Figure 4.** Cloud properties measured by the satellite and from the surface for high-level clouds (Figures 4a–4c; see text for restriction to large bias errors) and for midlevel clouds (Figures 4d–4f).

Figure 4. These correspond to the 21 midlevel cloud measurements shown in Figures 4d–4f, together with the 16 high-level cloud measurements shown in Figures 4a–4c that exhibit the largest biases (the five cases that exhibit close agreement with the models have been excluded). For midlevel clouds the surface-measured cloud amounts generally agree with the satellite cloud amounts (always 100%) quite well (Figure 4d). The column liquid water, as measured by the surface microwave radiometer, is also closely correlated with the satellite-measured infrared (IR) optical depth (Figure 4e). However, for high-level clouds the cloud amount and liquid water measured at the surface do not agree nearly as well with the satellite measurements (Figures 4a and 4b). With respect to the liquid water versus optical depth discrepancy (Figure 4b), the high cloud base (larger than 6 km) and the small optical depth (less than 1.2) mean that these are thin cirrus clouds and thus are primarily ice or mixed phase clouds since the environ-

mental temperatures are below  $-20^{\circ}\text{C}$ . This would explain the lack of correlation shown in Figure 4b, since the microwave radiometer measures only liquid water content and not ice content. Moreover, the amount of liquid water measured is close to the instrument resolution (0.03 mm). In order to identify the major causes of the biases shown in Figure 3 we have performed several sensitivity tests with the same soundings, but with different possible cloud inputs, and these are summarized in sections 5.2.1–5.2.4.

**5.2.1. Cloud height.** We first consider the dependence of OLR and SDLW upon cloud height. Since high-level (cirrus) clouds are optically thin, the physical cloud top is less radiatively significant than the height of the center of the cloud, termed the optical height, which represents the equivalent radiating height of the cloud [Minnis *et al.*, 1995]. Figure 4c shows that some cirrus clouds have higher physical tops than the cloud optical height, and for these clouds we distinguish in





**Figure 5.** CCM3 CRM sensitivity tests for perturbations of cloud height: High-level cloud (Figures 5a and 5b) and midlevel cloud (Figures 5c and 5d).

section 5.2.4 between their physical and optical cloud tops. For midlevel clouds the optical height is taken to be the cloud top height (physical height). Sensitivity tests of cloud height, using the CCM3 CRM, show that for a thin cirrus cloud the impact of cloud height on OLR is fairly small (Figure 5a). For the average of the 16 high-level cloud measurements the difference in moving the whole cloud layer up and down by 2 km is  $18 \text{ Wm}^{-2}$ , while for the SDLW the difference is only  $5 \text{ Wm}^{-2}$  (Figure 5b), largely because of the fact that high-level clouds have little impact on the SDLW because of the intervening atmosphere and the fact that they are cold and thus their downward emission is small. The optical depth for the average midlevel cloud is much larger than for the high-level clouds (Figures 4b and 4e). Therefore in the midlevel cloud cases the cloud heights have a much larger influence on the OLR and an even greater effect on SDLW because they are lower and warmer than for the high-level clouds. The difference in OLR and SDLW when the clouds are moved from +2 km to -2 km is  $40 \text{ Wm}^{-2}$  and  $31 \text{ Wm}^{-2}$ , respectively (Figures 5c and 5d).

**5.2.2. Cloud liquid water versus optical depth.** As emphasized in section 5.2, cloud liquid water as measured by the surface microwave radiometer for cirrus clouds is not representative of the cloud optical depth, which is dependent upon both cloud liquid water content and ice content. In CAGEX [Charlock and Alberta, 1996] the visible optical depth was converted into a cloud liquid water path which was then distributed throughout the model cloud. Alternatively, it is easy to modify the CCM2-CCM3 CRMs so as to directly input the IR optical depth, although there is still some uncertainty in this approach because of approximating the model's broadband longwave optical depth with the IR optical depth. CCM2 does not contain ice clouds, so cirrus clouds were treated as liquid

water clouds. In CCM3 the model determines the fraction of ice water from the total water according to the environmental temperature. We found the difference in OLR between CCM2 and CCM3 for these cirrus cases to be as large as  $16 \text{ Wm}^{-2}$  (CCM2 > CCM3) when the same amount of liquid water was employed in both models. If the optical depth is input instead of the liquid water, however, the difference is only  $4 \text{ Wm}^{-2}$  (CCM3 > CCM2). Thus the differentiation of ice clouds from liquid water clouds has improved the cirrus results by  $\sim 20 \text{ Wm}^{-2}$ .

**5.2.3. Cloud amount.** As shown in section 5.2, the cloud amount for thin overcast cirrus clouds as observed from the surface differs considerably from the satellite observations (Figure 4a). This raises a serious issue with respect to satellite versus lidar retrievals, as the nature of cirrus clouds is usually spatially inhomogeneous and transient [Mace *et al.*, 1998]. For satellite retrievals the threshold criteria using brightness temperature and visible reflectance of clear skies versus overcast skies is difficult to determine. If the threshold temperature is too high, then some of the clear pixels will be identified as overcast pixels [Minnis *et al.*, 1993]. Conversely, the micropulse lidar was reported to have missed many thin cirrus clouds for April 1994 (P. Minnis, personal communication, 2000). We address this and other issues in section 5.2.4.

**5.2.4. Sensitivity summary.** Figure 6a shows the average OLR and SDLW biases, relative to the measurements, of the CCM3 calculations for high-level clouds with different cloud input parameters as listed in Table 1. Recall that for high-level clouds the physical cloud top is the satellite-measured cloud top, while the optical cloud top is the height of the cloud center. For midlevel clouds, however, both refer to the satellite-measured cloud top. The lidar-measured cloud base height

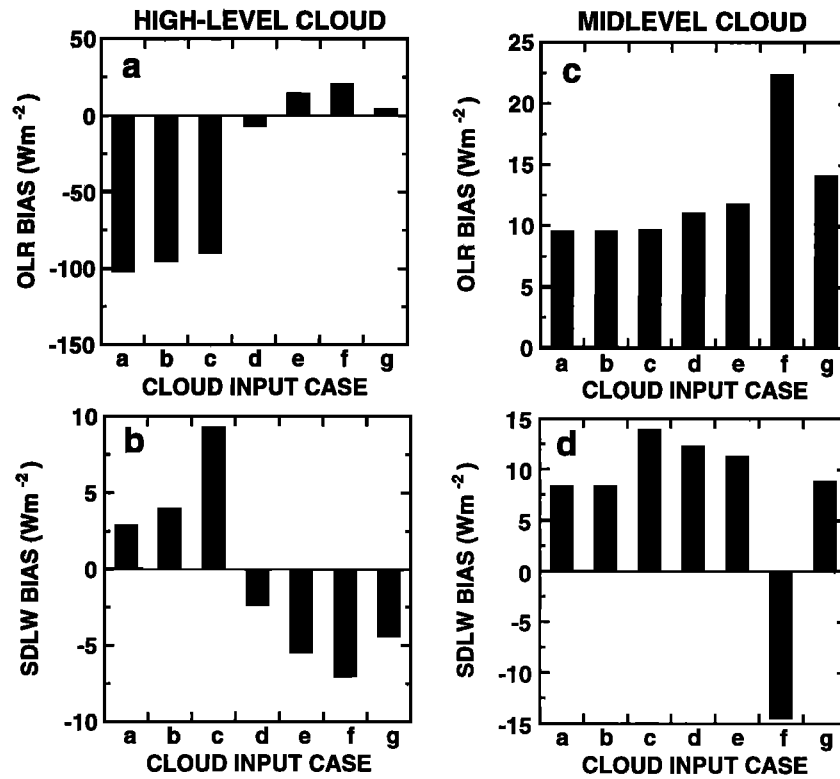


**Figure 6.** CCM3 CRM sensitivity tests for different cloud input parameters: High-level cloud (Figures 6a and 6b) and midlevel cloud (Figures 6c and 6d).

is used instead of the satellite-measured cloud base height for most of the cases summarized in Table 1, since it is regarded to be the more accurate of the two. Also, in Table 1, “liq” denotes using cloud liquid water measured by the surface microwave radiometer, while “opt” refers to the use of the IR optical depth measured by the satellite. The average OLR from the satellite retrieval for the 16 high-level cloud measurements of Figure 4 is  $247 \text{ Wm}^{-2}$ . The CCM3 calculations for cases a, b, and c are  $90\text{--}100 \text{ Wm}^{-2}$  lower than this (Figure 6a), which is obviously caused by employing only cloud liquid water content. However, using the observed IR optical depth (cases d and e) improves the result significantly, since this includes both liquid water and ice contents. The difference between cases d and e is  $\sim 20 \text{ Wm}^{-2}$ , which is caused by differences in cloud amount; case e employs the surface-measured cloud amount. However, when both OLR and SDLW (Figure 6b) are compared to the measurements, the satellite-measured cloud amount produces a better overall result. Yet we cannot actually conclude that the satellite provides better measurements than the lidar, since the two cloud amounts have different statistical content. The satellite cloud products (cloud amount, OLR, and optical depth)

are consistent with each other; only the surface fluxes are independent measurements.

Although the satellite retrievals used the plane-parallel, nonoverlapping assumption, so that there was no overlap between different cloud layers (among high-level, midlevel, and low-level clouds), there is no indication as to whether in the same satellite layer (which may consist of multiple model layers) we should consider overlap or not. The computational treatment actually used the maximum overlap assumption, since we gave each model layer 100% cloud amount. In cases f and g we tried different cloud overlap assumptions. Case f uses the nonoverlapping assumption, so that each model layer has only a fraction of the total cloud amount. In case g the random overlap assumption was used as in the original CCM. Figure 6a shows that for cirrus clouds the different cloud overlap assumptions can affect the OLR by as much as  $20 \text{ Wm}^{-2}$ . For midlevel clouds it can also affect SDLW by more than  $20 \text{ Wm}^{-2}$  (Figure 6d). Overall, the random overlap assumption seems to be the preferable procedure, although in these cases it is close to maximum overlap because for 100% cloud cover each model layer has a large cloud fraction.

**Table 1.** Input Cirrus Cloud Information for CCM3 CRM

	Case a	Case b	Case c	Case d	Case e	Case f	Case g
Cloud top	physical	optical	optical	optical	optical	optical	optical
Cloud base	satellite	satellite	surface	surface	surface	surface	surface
Liq/opt <sup>a</sup>	liq	liq	liq	opt	opt	opt	opt
Cloud amount	satellite	satellite	satellite	satellite	surface	nonoverlap	random overlap

<sup>a</sup>Liq, cloud liquid water measured by the surface microwave radiometer was used; opt, IR optical depth measured by the satellite was used.

**Table 2.** Cloud Overlap Assumptions for CCM3 CRM

	Case a	Case b	Case c	Case d	Case e	Case f	Case g	Case h
Cloud overlap	maximum overlap	random overlap	nonoverlap	late overlap	maximum overlap	random overlap	nonoverlap	late overlap
Liq/opt	liq	liq	liq	liq	opt	opt	opt	opt

### 5.3. CCM2-CCM3 Column Radiation Models: All Skies

The all-sky cases include not only clear and overcast conditions but also multilayer clouds. The cloud overlap assumptions can result in an uncertainty of  $14 \text{ Wm}^{-2}$  for the global SDLW and  $30 \text{ Wm}^{-2}$  for the regional SDLW when applying International Satellite Cloud Climatology Project (ISCCP) cloud data to a radiation model [Charlock *et al.*, 1993], so it is important that the overlap assumptions be chosen carefully. Here we will test different cloud overlap assumptions to determine which assumption is the best for the CCM2-CCM3 CRM.

CAGEX used the nonoverlapping assumption following the satellite retrieval method so that the total flux for a grid is calculated from separate clear-sky and overcast conditions (T. Alberta, personal communication, 1998). If there are 10% low-level, 20% midlevel, and 30% high-level clouds, four separate calculations are made, and the flux is summed as follows:  $\text{FLUX} = 0.1 \text{ LOW} + 0.2 \text{ MID} + 0.3 \text{ HIGH} + 0.4 \text{ CLEAR}$ . Alternatively, in the CCM2-CCM3 CRM the cloud fraction can be incorporated into the cloud emissivity formula for each model layer, as in the CCM2-CCM3 general circulation models, so there is only one calculation for each grid no matter how the clouds are vertically distributed.

For cases with multiple layers of satellite clouds the non-overlapping assumption is used between different cloud layers as the satellite has provided separate cloud properties for each layer. Within each layer, three overlap assumptions are applied to the corresponding model layers: maximum (complete) overlap (case a), random overlap (case b) and nonoverlap (case c), as summarized in Table 2. Another test to mimic the pure radiation code is to run the code up to 4 times for clear conditions and 100% cloud for each cloud layer, then sum up the separate fluxes (we refer to this as “late overlap”) as is done in case d. These cases use the surface-observed cloud liquid water amount. The other set of tests (cases e–h) follow

the same cloud overlap assumptions but with the input of the direct IR optical depth.

The observed cloud liquid water comprises half-hour averages, and it differs from the model-defined cloud water path, which refers to the cloud water content of the cloud body, so it was necessary to recalculate the cloud water path for each model layer and with each cloud overlap assumption. If uniform cloud density  $\rho$  is assumed, then

$$\sum_i \Delta P_i \rho \text{CLDFRC}_i = \text{LIQ}, \quad (1)$$

$$\Delta Q_i = \Delta P_i \rho, \quad (2)$$

where LIQ is the observed column liquid water,  $\Delta P_i$  is the cloud thickness in pressure units, and  $\Delta Q_i$  is the cloud liquid water path for model layer  $i$ .  $\text{CLDFRC}_i$  is the cloud fraction which is decided by the satellite cloud amount ( $\text{CLD}_i$ ) and the cloud overlap assumptions

Maximum overlap

$$\text{CLDFRC}_i = \text{CLD}_l,$$

Random overlap

$$\text{CLDFRC}_i = 1 - (1 - \text{CLD}_l)^{1/N_l},$$

Nonoverlap

$$\text{CLDFRC}_i = \text{CLD}_l / N_l,$$

where  $l$  refers to the three satellite cloud layers (high, middle, and low) and  $N_l$  is the number of model layers each satellite layer occupies.

The sensitivity results are summarized in Figure 7 and represent the average of 154 individual measurements. Clearly, the set of cases which utilize the input of cloud liquid water (cases a through d) still have larger biases, relative to the

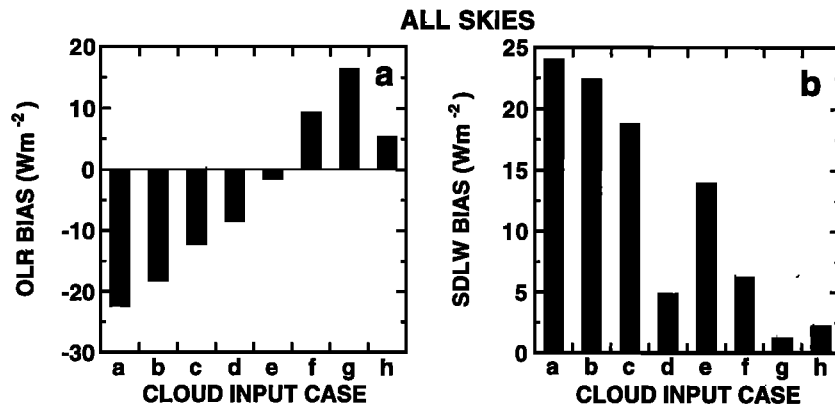


**Figure 7.** CCM3 CRM sensitivity tests for different cloud overlap assumptions: (a) OLR bias and (b) SDLW bias.

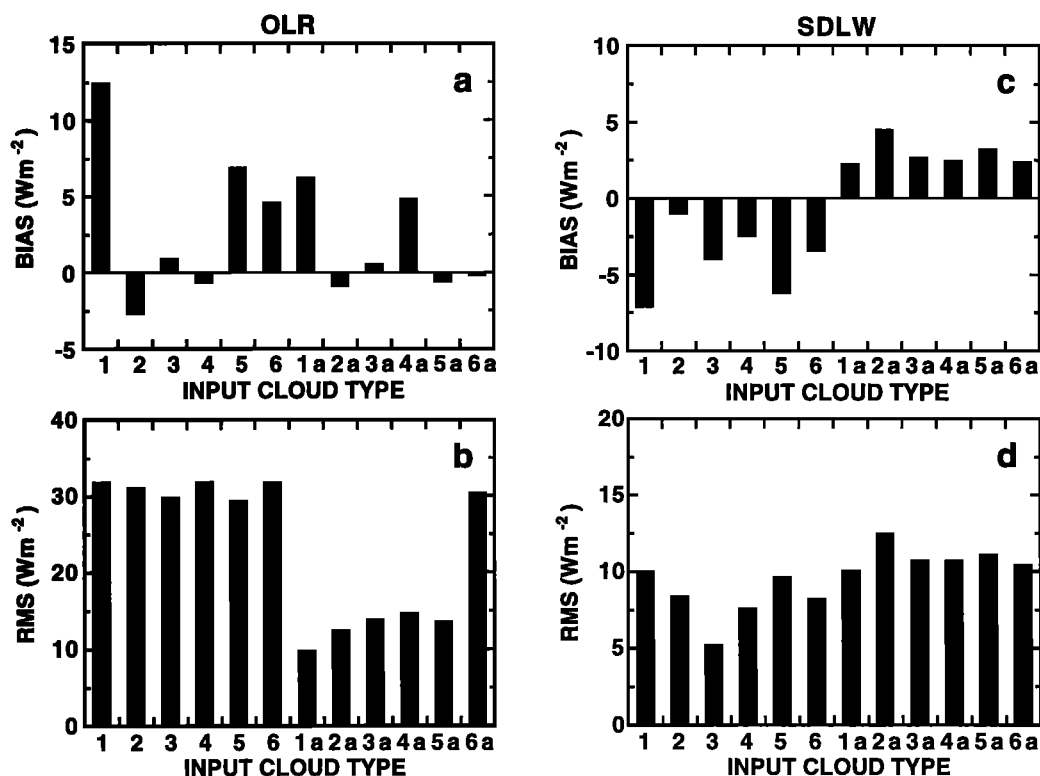


**Figure 8.** MODTRAN bias and RMS errors with respect to the choice of different model cloud types. OLR (Figures 8a and 8b) and SDLW (Figures 8c and 8d).

measurements, than for the optical depth input (cases e through h) for both OLR and SDLW. The differences resulting from the cloud overlap assumptions are larger for the OLR (over  $20 \text{ Wm}^{-2}$ ) than for the SDLW ( $\sim 15 \text{ Wm}^{-2}$ ). The maximum overlap assumption (case e) results in the maximum cloud amount and the minimum cloud water path for each model layer, while the nonoverlap assumption (case g) leads to the minimum cloud amount and the maximum cloud water path. Although these two effects partially compensate each other, from Figure 7 it is obvious that the SDLW gradually decreases and OLR increases as the cloud amount decreases (case g relative to case e), which means that cloud amount is more important than cloud water content in affecting the long-wave fluxes. It is interesting to note that case h, which considers cloud overlap after the calculations, produces the best overall results (both OLR and SDLW).

#### 5.4. MODTRAN3 Radiation Model

MODTRAN3 provides more flexibility with user-defined cloud and optical properties than do the CCM2-CCM3 CRMs.

**Table 3.** Properties of the MODTRAN Cumulus- and Stratus-Type Model Clouds

Cloud	Cloud Type	Thickness, km	Base, km	$0.55 \mu\text{m}$ Extinction, $\text{km}^{-1}$	Column Amount, $\text{kg g m}^{-3}$
1	cumulus	2.34	0.66	92.6	1.6640
2	altostratus	0.60	2.40	128.1	0.3450
3	stratus	0.67	0.33	56.9	0.2010
4	stratus/stratocumulus	1.34	0.66	38.7	0.2165
5	nimbostratus	0.50	0.16	92.0	0.3460

It allows users to choose from five internal cumulus and stratus cloud models and two cirrus models. It is also possible to modify the default cloud with user input cloud extinction and absorption coefficients at certain wavelengths. The cloud profile, including cloud base, thickness, and cloud liquid and ice water amounts can also be modified with a custom set of optical parameters. The bulk properties observed from various instruments for the CART site include cloud height information, visible and infrared optical depth, and column liquid water. Since these variables alone cannot determine what kind of cloud it is, and there are no direct measurements of detailed optical properties, the best way to describe the real cloud in the model is to input as many observed variables as possible and choose from model defaults for those unknown quantities. In this case, we specify the cloud height and column liquid water using observations and choose the optical parameters from the default models. Although optical depth is not a direct input parameter, it is used to compute the extinction coefficient together with the cloud thickness, so that in equivalence, the cloud optical depth in the model is constrained by the observations.

Figure 8 shows the bias and RMS errors of the MODTRAN3 calculations for the 46 one-layer overcast satellite cloud cases during the April 1994 IOP with different default cloud optical properties. Cases 1–5 represent five default cloud types for which the observed cloud liquid water was used as input to the model, and the properties of these cloud types are listed in Table 3. In case 6 the cirrus cloud type was chosen for clouds higher than 6 km, while a stratus/stratocumulus cloud (type 4) was chosen for other clouds. Cases 1a–6a repeat the cloud types, but adjust the extinction coefficient so as to be constrained with the observed IR optical depth. The large bias errors of SDLW and OLR for cloud type 1 indicate that cu-

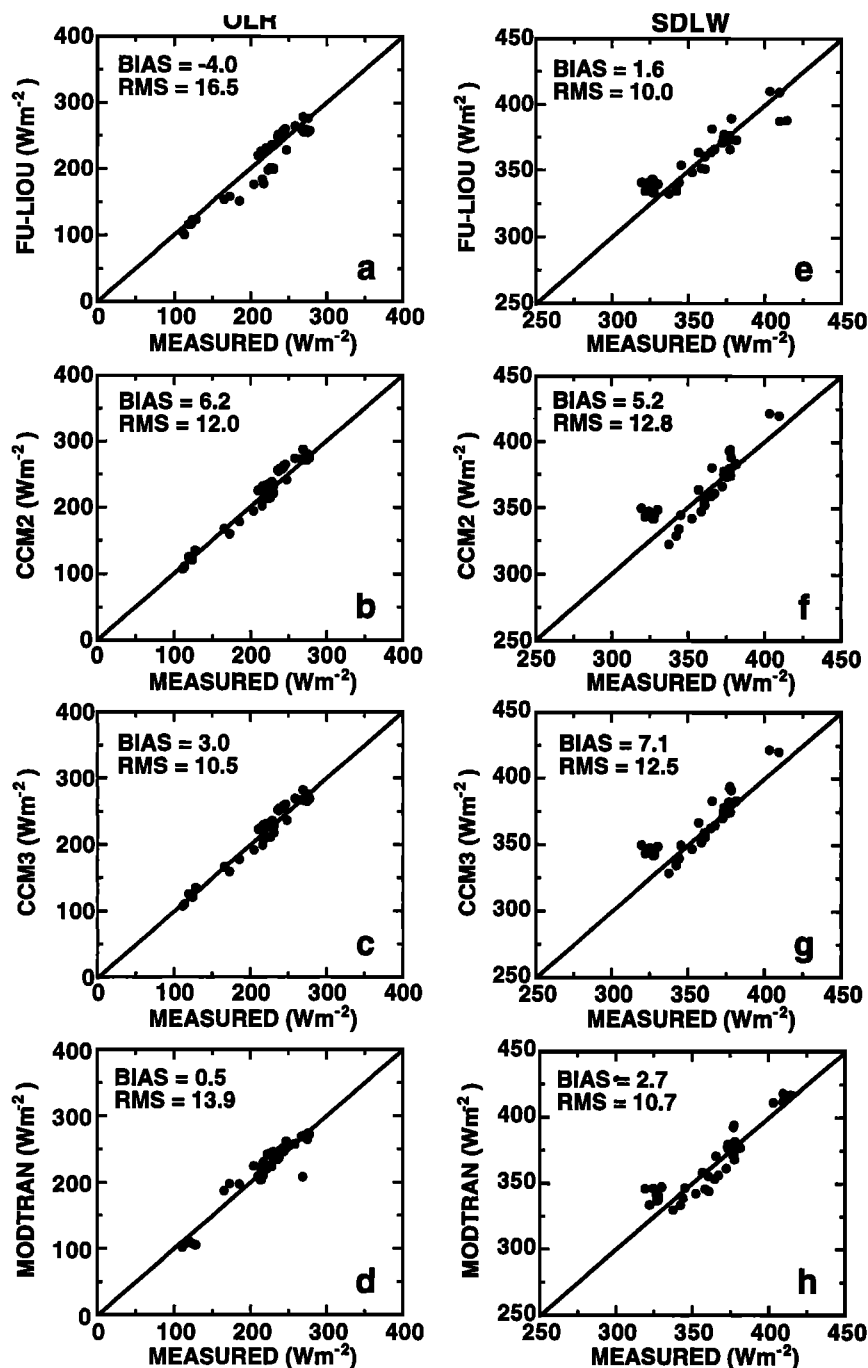


**Figure 9.** Comparison of the four models to measurements for overcast skies: OLR (Figures 9a–9d) and SDLW (Figures 9e–9h). See text for an explanation of cloud input parameters.

mulus clouds are not the typical cloud type for spring in Oklahoma. Using stratus cloud types 2, 3, and 4 produces considerably better results. The large RMS error for OLR is also improved by employing the observed optical depth.

Figure 9 compares the MODTRAN3 cloud (with assumed stratus cloud type, case 3a) calculations to the other three models. The bias and RMS errors are for all 46 overcast cloud cases, and the calculations using the Fu-Liou code are the same CAGEX calculations as shown in Figures 3a and 3d. The CCM2-CCM3 calculations employ the case d input parameters from Table 1, in contrast to the case a parameters used in Figure 3. The MODTRAN3 calculations give the best overall

estimates of both OLR and SDLW, although the Fu-Liou model and the CCM3 CRM are both in quite reasonable agreement with the measurements. An interesting point is that the  $7 \text{ Wm}^{-2}$  difference between the CCM3 and Fu-Liou OLR biases (Figure 9c versus 9a) coincides, as discussed in section 3, with the fact that cloud scattering causes a  $6 \text{ Wm}^{-2}$  reduction in OLR within the Fu-Liou model [Fu et al., 1997].

## 6. Summary and Discussion

Data taken at the Atmospheric Radiation Measurement Program's central facility in Oklahoma and processed as part

of the Clouds and the Earth's Radiant Energy System-Atmospheric Radiation Measurement-Global Energy and Water Cycle Experiment (CAGEX) project Oklahoma [Charlock and Alberta, 1996], have been used to validate the top-of-the-atmosphere and surface longwave radiative fluxes for two widely used radiation models: the Column Radiation Model from the National Center for Atmospheric Research Community Climate Model (CCM) and the Moderate Resolution Transmittance (MODTRAN3) radiation code. For completeness we have also included in these comparisons the CAGEX-computed fluxes using the Fu-Liou radiation model [Fu and Liou, 1992].

The clear-sky results show some systematic underestimates of SDLW and overestimates of OLR for all models. However, one should not conclude that the models actually underestimate the greenhouse (SDLW minus OLR) effect, since we cannot exclude the possibility of insufficient input of absorbing gases. For example, the upper atmospheric water vapor is highly suspect.

For overcast skies an important issue to resolve when using a point-to-point radiative transfer model to represent a grid-averaged atmospheric state and radiative fluxes is to correctly collocate the various measurements taken from the satellite instruments, the surface instruments, and the sounding profiles. The TOA-surface collocation problem, in terms of cloud measurements, was illustrated using cloud amount and base height as measured both by the satellite and from the surface. Results from this study show that the cloud parameters taken from satellite spatial averages and surface temporal averages have large discrepancies when considered case by case. Moreover, a crucial mistake in using the surface microwave radiometer to measure cloud liquid water content is that this biases the cirrus cloud measurements, since the microwave radiometer cannot measure ice water content. Conversely, the satellite retrievals of IR optical depth (which includes both liquid and ice water content) are very useful, not only in their large area coverage, but also for more accurate high cirrus cloud information. On the other hand, the satellite technique has its own limitations, such as poor treatment of multilayer clouds.

In order to apply satellite cloud amount to the models a cloud overlap assumption is necessary. Different overlap assumptions can result in differences in OLR and SDLW of the order of 15 and 20  $\text{W m}^{-2}$ , respectively, for the April 1994 IOP alone. Thus more accurate cloud profiling and overlap information are highly desired for this purpose. In addition, radar and aircraft have the potential to provide three-dimensional cloud geometry information.

**Acknowledgments.** We are grateful to the following individuals for their advice and assistance: Marvin Geller, Minghua Zhang, and Duane Waliser of SUNY Stony Brook; Patrick Minnis, Thomas Charlock, and Tim Alberta of NASA Langley Research Center; Mark Miller and Joyce Tichler of Brookhaven National Laboratory; James Lilegren and Marvin Wesley of the ARM Data Center; and Ruchong Yu of the Institute of Atmospheric Physics, Chinese Academy of Sciences. This work was supported by the DOE ARM Program through grant DEFG0290ER61063, by DOE grant DEFG0285ER60314, and by the CERES Project through NASA contract NAS1-981421, all to SUNY Stony Brook.

## References

Abreu, L. W., and G. P. Anderson, The MODTRAN 2/3 report and LOWTRAN 7 model, Air Force Phillips Lab., Geophys. Dir., Hanscom Air Force Base, Mass., 1996.

- Acharya, P. K., S. M. Adler-Golden, G. P. Anderson, A. Berk, L. S. Bernstein, J. H. Chetwynd, and M. W. Matthew, MODTRAN version 3.7/4.0 users' manual, Air Force Res. Lab., Space Vehicle Dir., Air Force Mater. Command, Hanscom Air Force Base, Mass., 1998.
- Cess, R. D., et al., Absorption of solar radiation by clouds: Observations versus models, *Science*, 267, 496-499, 1995.
- Cess, R. D., M. H. Zhang, Y. Zhou, X. Jing, and V. Dvortsov, Absorption of solar radiation by clouds: Interpretations of satellite, surface, and aircraft measurements, *J. Geophys. Res.*, 101, 23,299-23,309, 1996.
- Charlock, T. P., and T. L. Alberta, The CERES/ARM/GEWEX experiment (CAGEX) for the retrieval of radiative fluxes with satellite data, *Bull. Am. Meteorol. Soc.*, 77, 2673-2683, 1996.
- Charlock, T. P., F. Rose, T. Alberta, G. L. Smith, D. Rutan, N. Manalo-Smith, P. Minnis, and B. Wielicki, Cloud profiling radar requirements: Perspective from retrievals of the surface and atmospheric radiation budget and studies of atmospheric energetics, paper presented at GEWEX Topical Workshop on Utility and Feasibility of a Cloud Profiling Radar on TRMM-2, Jet Propul. Lab., Pasadena, Calif., June 29 to July 1, 1993.
- Chou, M. D., and W. Zhao, Estimation and model validation of surface solar radiation and cloud radiative forcing using TOGA COARE measurements, *J. Clim.*, 10, 610-620, 1997.
- d'Almeida, G. A., P. Koepke, and E. P. Shettle, *Atmospheric Aerosols: Global Climatology and Radiative Characteristics*, 561 pp., A. Deepak, Hampton, Va., 1991.
- Doelling, D. R., W. L. Smith Jr., P. Minnis, and F. P. J. Valero, Broadband radiation fluxes from narrowband radiances, paper presented at ALPS 99 Conference, Cent. Natl. d'Etud. Spatiales, Meribel, France, Jan. 18-22, 1999.
- Ellingson, R. G., J. Ellis, and S. Fels, The intercomparison of radiation codes used in climate models: Longwave results, *J. Geophys. Res.*, 96, 8929-8953, 1991.
- Fu, Q., and K.-N. Liou, On the correlated  $k$ -distribution method for radiative transfer in nonhomogeneous atmospheres, *J. Atmos. Sci.*, 49, 2139-2156, 1992.
- Fu, Q., K. N. Liou, M. C. Cribb, T. P. Charlock, and A. Grossman, Multiple scattering parameterization in thermal infrared radiative transfer, *J. Atmos. Sci.*, 54, 2799-2812, 1997.
- Han, D., and R. G. Ellingson, An experimental technique for testing the validity of cumulus cloud parameterizations for longwave radiation calculations, *J. Appl. Meteorol.*, 39, 1147-1159, 2000.
- Kandel, R. S., J. L. Monge, M. Violler, L. A. Pakhomov, V. I. Adasko, R. G. Reitenbach, E. Raschke, and R. Stuhlmann, The ScaRaB project: Earth radiation observations from the Meteor satellites, *Adv. Space Res.*, 14(1), 47-54, 1993.
- Kiehl, J. T., and B. P. Briegleb, A new parameterization of the absorptance due to the 15  $\mu\text{m}$  band system of carbon dioxide, *J. Geophys. Res.*, 96, 9013-9019, 1991.
- Kiehl, J. T., J. J. Hack, and B. P. Briegleb, The simulated Earth radiation budget of the NCAR CCM2 and comparison with the Earth Radiation Budget (ERBE), *J. Geophys. Res.*, 99, 20,815-20,827, 1994.
- Kiehl, J. T., J. J. Hack, G. B. Bonan, B. A. Boville, B. P. Briegleb, D. L. Williamson, and P. J. Rasch, Description of the NCAR Community Climate Model (CCM3), *NCAR Tech. Note NCAR/TN-420+STR*, Natl. Cent. for Atmos. Res., Boulder, Colo., 1996.
- Kneizys, F. X., E. P. Shettle, L. W. Abreu, J. H. Chetwynd, G. P. Anderson, W. O. Gallery, J. E. Selby, and S. A. Clough, Users guide to LOWTRAN 7, *Tech. Rep. AFGL-TR-88-0177*, U.S. Air Force Geophys. Lab., Hanscom Air Force Base, Mass., 1988.
- Long, C. N., and T. P. Ackerman, Surface measurements of solar irradiance: A study of the spatial correlation between simultaneous measurements at separated sites, *J. Appl. Meteorol.*, 34, 1039-1046, 1995.
- Mace, G. G., T. P. Ackerman, P. M. Minnis, and D. F. Young, Cirrus layer microphysical properties derived from surface-based millimeter radar and infrared interferometer data, *J. Geophys. Res.*, 103, 23,207-23,216, 1998.
- Minnis, P., P. W. Heck, and D. F. Young, Inference of cirrus cloud properties using satellite-observed visible and infrared radiances, part II, Verification of theoretical cirrus radiative properties, *J. Atmos. Sci.*, 50, 1305-1322, 1993.
- Minnis, P., W. L. Smith Jr., D. P. Garber, J. K. Ayers, and D. R. Doelling, Cloud properties derived from GOES-7 for spring 1994

- ARM Intensive Period using version 1.0.0 of ARM Satellite Data Analysis Program, *NASA Ref. Publ.*, 1366, 1995.
- Ramanathan, V., and R. E. Dickinson, The role of stratospheric ozone in the zonal and seasonal radiative energy balance of the Earth-troposphere system, *J. Atmos. Sci.*, **36**, 1084–1104, 1979.
- Ramanathan, V., and P. Downey, A nonisothermal emissivity and absorptivity formulation for water vapor, *J. Geophys. Res.*, **91**, 8649–8666, 1986.
- Roberts, R. E., J. E. A. Selby, and L. M. Biberman, Infrared continuum absorption by atmospheric water vapor in the 8–12 micron window, *Appl. Opt.*, **15**, 2085–2090, 1976.
- Rothman, L. S., et al., The HITRAN molecular database: Edition of 1991 and 1992, *J. Quant. Spectrosc. Radiat. Transfer*, **48**, 469–507, 1992.
- Slingo, J. M., The development and verification of a cloud prediction scheme for the ECMWF model, *Q. J. R. Meteorol. Soc.*, **113**, 899–927, 1987.
- Slingo, A., and M. Webb, Simulation of clear sky outgoing longwave radiation over the oceans using operational analyses, *Q. J. R. Meteorol. Soc.*, **118**, 1117–1144, 1992.
- Smith, G. L., R. N. Green, E. Raschke, L. M. Davis, J. T. Suttles, B. A. Wieliki, and R. Davies, Inversion methods for satellite studies of the Earth's radiation budget: Development of algorithms for the ERBE mission, *Rev. Geophys.*, **24**, 407–421, 1986.
- Spinhrne, J. D., Micro pulse lidar, *IEEE Trans. Geosci. Remote Sens.*, **31**, 48–55, 1993.
- Stokes, G. M., and S. Schwartz, The Atmospheric Radiation Measurement (ARM) Program: Programmatic background and design of the cloud and radiation test bed, *Bull. Am. Meteorol. Soc.*, **75**, 1201–1221, 1994.
- Susskind, et al., Characteristics of the TOVS pathfinder path A dataset, *Bull. Am. Meteorol. Soc.*, **78**, 1449–1472, 1997.
- Waliser, D. E., W. D. Collins, and S. P. Anderson, An estimate of surface shortwave cloud forcing over the western Pacific during TOGA COARE, *Geophys. Res. Lett.*, **23**, 519–522, 1996.
- Wielicki, B. A., and the CERES Science Team, *Clouds and the Earth's Radiant Energy System (CERES) Algorithm Theoretical Basis Document*, vol. 2, *Geolocation, Calibration, and ERBE-like Analyses (Subsystems 1–3)*, *NASA Ref. Publ.*, 1376, 119 pp., Dec. 1995.
- Wild, M., A. Ohmura, A. Gilgen, and E. Roeckner, Regional climate simulation with a high-resolution CM: Surface radiative fluxes, *Clim. Dyn.*, **11**, 469–486, 1995.

---

R. D. Cess, Marine Sciences Research Center, State University of New York, Stony Brook, NY 11794-5000. (rcess@notes.cc.sunysb.edu)  
 Y. P. Zhou, Analytical Services & Materials, Inc., One Enterprise Parkway, #300, Hampton, VA 23666-5845.

(Received March 16, 2000; revised July 7, 2000;  
 accepted August 29, 2000.)